Ag@*g*-C_3N_4 Nanocomposite: an Efficient Catalyst Inducing the Reduction of 4-Nitrophenol①

LIU Min-Min[a] YING Shao-Ming[b] CHEN Bao-Guo[c]
GUO Hong-Xu[a②] HUANG Xu-Guang[a]

[a] (*College of Chemistry, Chemical Engineering and Environment, Minnan Normal University, Zhangzhou* 363000, *China*)

[b] (*Fujian Provincial Key Laboratory of Featured Materials in Biochemical Industry, College of Chemistry and Materials, Ningde Normal University, Ningde* 352100, *China*)

[c] (*International College, Krirk University, Bangkok* 10220, *Thailand*)

ABSTRACT In this study, an efficient catalyst Ag@*g*-C_3N_4 nanocomposite was successfully synthesized through a simple green reaction, and the characterizations through XRD, FTIR, SEM, BET and XPS were also studied. The activities of Ag@*g*-C_3N_4 were investigated toward the reduction of 4-nitrophenol to their corresponding aminophenol compounds in the presence of excess $NaBH_4$ as a reducing agent. The Ag@*g*-C_3N_4 nanocomposites exhibited high catalytic activities, in which a 92.2% 4-nitrophenol conversion in 10 min and the apparent rate constant K_{app} = 264.27×10^{-3} min^{-1} were obtained. The as-prepared Ag@*g*-C_3N_4 nanocomposites showed great potential in catalytically inducing the reduction of 4-nitrophenol, which makes them economically and energy conservation attractive from industrial waste water treatment.

Keywords: Ag@*g*-C_3N_4, catalytic activities, the reduction of 4-nitrophenol, cycle experiment;
DOI: 10.14102/j.cnki.0254-5861.2011-3178

1 INTRODUCTION

With the rapid economic development, the living environment has encountered arduous challenge. The water resource has been severely polluted by domestic wastewater, medical wastewater and uncontrolled industrial pollution. Phenolic compounds are one of the model pollutants, one of the most common toxic pollutants in the pharmaceutical industry, the wastewater of dye industry[1]. Among them, the 4-nitrophenol (4-NP) and its derivatives are one of the major organic pollutants of phenolic compounds. In addition, 4-NP and its derivatives are mutagenic, carcinogenic and toxic with an inhibitory nature. They are considered as a hazardous material because of their increased discharge in water that affects human and animal life[2]. Up to now, various technologies (adsorption[3], photocatalytic degradation[4], ozonation[5] and catalytic reduction[6]) have been explored to removal the toxic nitroaromatics. Compared with them, the catalytic reduction process is a very simple and efficient method to convert toxic nitrophenol (NP) to benign aminophenol (AP). Furthermore, aminophenols obtained from the reduction of nitrophenols are essential industrial chemicals used as a precursor and an intermediate in the synthesis of many drugs and other high value-added chemical products[7]. Thus, it is very desirable to produce a cost-effective and highly stable efficient catalyst for the reduction of nitro-compounds under mild conditions.

Noble metal nanoparticles (Au, Ag, Pt and Pd) show distinctive catalytic properties due to their high surface areas and surface-to-volume ratios. However, in order to commercialize such catalysts, we should consider the two key criteria, their cost effectiveness and efficiency. For achieving both criteria, we can take the noble metals with other less expensive non-noble metals, which may reduce the amount of the former and provide cost-effective catalysts. As we all know, graphitic carbon nitride (*g*-C_3N_4) with a suitable visible

Received 30 March 2021; accepted 27 April 2021

① Project supported by the Natural Science Foundation of Fujian Province (No. 2019J01747 and 2020J01803), Fujian Provincial Key Laboratory of Featured Materials in Biochemical Industry (FJKL_FBCM202104) and China NSF (No. 41976150)

② Corresponding author. Prof. Guo Hong-Xu, received Ph. D in physical chemistry from Fuzhou University in 2006. E-mail: guohx@mnnu.edu.cn

lightdriven band gap (2.7 eV) is a metal-free polymeric photocatalyst, which has been considered to be a safe catalyst[8]. Doping of *g*-C_3N_4 with noble metallic ions would be more efficient in improving the photocatalytic activity for the degradation of organic pollutants in wastewater. This is mainly due to the ability of electron capture by these noble metallic ions, around which the photo generated electrons aggregate, giving rise to a higher separation of photo generated electrons and holes[9]. These were some reports utilized directly calcined *g*-C_3N_4 solid to prepare silver and *g*-C_3N_4 nanocomposites, which could effectively degrade the organic dyes such as methyl orange[10] and methylene blue[11]. However, systematic study on Ag nanoparticles deposited on porous *g*-C_3N_4 nanostructure for catalytic reduction of nitrophenol has seldom been reported[12].

In this study, *g*-C_3N_4 was fabricated through a thermal co-poly-condensation procedure, and Ag nanoparticle was modified on the interlayers and surface of *g*-C_3N_4. The characterizations of the as-synthesized catalysts were carried out by XRD, FT-IR, SEM, BET and XPS techniques. UV-*vis* spectrophotometry was used to record continuously the conversion rates of 4-NP to the 4-AP compound. And the kinetics of 4-NP degradation was also studied, which follows the pseudo-first-order equation. This study indicated that the as-prepared Ag@*g*-C_3N_4 nanocomposite is a kind of excellent catalyst for the reduction of 4-NP in mild reaction, which makes them economically and energy conservation attractive for the removal of 4-NP from industrial waste water treatment.

2 EXPERIMENTAL

2. 1 Synthesis of Ag@*g*-C_3N_4

All reagents were obtained from commercial sources and used without further purification.

2. 1. 1 Preparation of *g*-C_3N_4

First, melamine (5.000 g) and carbamide (5.000 g) were mixed and grounded for 15 min at room temperature. As a result, a white colored powder was obtained, which was transferred into a crucible with cover and heated at 500 ℃ for 4 h with a ramp rate of 3 ℃/min for the heating processes in muffle furnace (SX2-2.5-12GP, Jinan Yudian, China). Then, the obtained pale yellow product was washed with water and ethanol for 3 times. Finally, the product *g*-C_3N_4 was obtained after vacuum drying for 10 h at 80 ℃.

2. 1. 2 Preparation of Ag@*g*-C_3N_4

A solution of $AgNO_3$ (0.050 g) in 10 mL of deionized (DI) water was gradually added to the *g*-C_3N_4 solution (0.500 g dispersed in 50 mL of DI water) to get the mixed solution, which was stirred continuously for 4 h at 1000 rpm in natural light. After that the precipitate was separated by centrifugation to get the crude brown product, then the impurities were removed by water washing for three times and the final brown product Ag@*g*-C_3N_4 was obtained by vacuum drying for 4 h.

2. 2 Structure determination

X-ray diffraction (XRD) measurement was carried out on a Bruker D8 Advance diffractometer with Cu*Kα* radiation (scanned range: 5～60°, scan rate: 8 °/min). Fourier transform infrared (FT-IR) spectra were recorded in the range of 400～4000 cm^{-1} with 2 cm^{-1} resolution on a Nicolet 6700 FTIR spectrometer using the KBr pellet technique (1 mg of the sample in 100 mg of KBr). Scanning electron microscopy (SEM) was conducted with a Thermo Fisher (FEI) Helios G4 CX microscope and energy dispersive X-ray spectrometer (EDX) elemental mapping was conducted with a Bruker XFlash 6|60 microscope. X-ray photo-electron spectroscopy (XPS) was performed on a Thermo Scientific K-Alpha spectrometer with Al*Kα* radiation (Analyser Mode: CAE, full-spectra: 100 eV, narrow-spectra: 50 eV, Spot Size: 400*μ*m). Brunauer-Emmett-Teller (BET) method for surface area and porosity analysis was performed on a Specific Surface Area and Porosity analyzer (Gemini Ⅶ Serial#340, micromeritics, USA).

2. 3 Catalytic reduction

The as-prepared Ag@*g*-C_3N_4 composite was used as the catalyst for 4-NP reduction with $NaBH_4$ and without stirring. In this reaction, 4-NP was converted to phenolate ion species with the help of existence of $NaBH_4$. In a typical experiment, 1 mL of 4-NP aqueous solution (0.1 mM), 3.0 mg $NaBH_4$ and 0.01 mL of Ag@*g*-C_3N_4 suspension (0.5 mg/mL) were sequentially added into a standard quartz cell. Then, UV-vis spectroscopy (UV-1600PC, Shanghai Mapada Instruments) was used to trace the 4-NP reduction reaction of the mixture interval one minute.

The Ag@*g*-C_3N_4 nanocomposite used in the catalytic reduction reaction was recycled and repeatedly used for 3 cycles to examine the cycling stability. After each cycle, the Ag@*g*-C_3N_4 was collected by centrifugal separation.

3 RESULTS AND DISCUSSION

The XRD patterns of *g*-C_3N_4 and Ag@*g*-C_3N_4 are shown in Fig. 1a. Two diffraction peaks at 13.1 ° and 27.5 ° correspond to the crystal characteristics of (100) and (002) of layered *g*-C_3N_4[13-15]. Because of the small loading of Ag ion in *g*-C_3N_4, no significant diffraction peaks corresponding to Ag were observed. The FT-IR spectra of *g*-C_3N_4 and Ag@*g*-C_3N_4 are shown in Fig. 1b. The peak around 810 cm^{-1} belongs to the respiratory vibration pattern of tri-s-triazine ring[16]. Those intensive absorption peaks in the range of 1200～1680 cm^{-1} can be classified to the different vibration modes of C-N bond involved in the tri-s-triazine heterocycles[17]. The wide peak of 3000～3500 cm^{-1} was attributed to the stretching vibration of N–H and O–H[18].

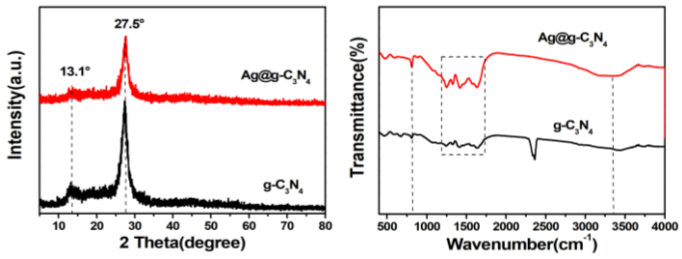

(a) **(b)**

Fig. 1. (a) XRD patterns and (b) FTIR spectra of the as-prepared *g*-C_3N_4 and Ag@*g*-C_3N_4

The SEM images of as-synthesized *g*-C_3N_4 and Ag@*g*-C_3N_4 samples are shown in Fig. 2. From the low magnification SEM image (Fig. 2a), it can be seen that the micro-morphology of *g*-C_3N_4 is a porous block with rough surface. After Ag loading modified *g*-C_3N_4, its micro-morphology did not change greatly (Fig. 2b). The high-magnification SEM image shows that the porous lumps are formed by the accumulation of nano-sheets of different sizes. From EDS images (Fig. 2c), we can see that the Ag@g-C_3N_4 sample contains three elements of C, N, and Ag, and the Ag element is uniformly distributed in the sample, indicating that Ag nanoparticle was successfully loaded on the surface of *g*-C_3N_4 by liquid phase reduction deposition.

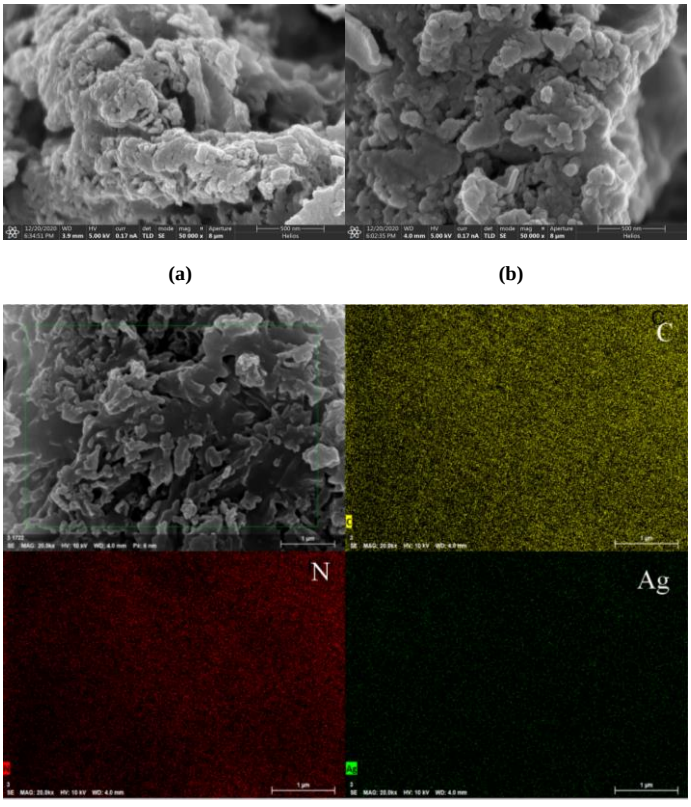

(a) **(b)**

(c)

Fig. 2. SEM images of (a) *g*-C_3N_4 and (b) Ag@*g*-C_3N_4; (c) EDX elemental mapping image of Ag@*g*-C_3N_4

Chemical state and chemical composition of Ag@g-C_3N_4 sample have been measured by X-ray photoelectron spectroscopy (XPS). Fig. 3a shows the full spectra of Ag@g-C_3N_4 sample, in which three elements of C, N and Ag are detected. The full spectra analysis confirmed that Ag was successfully modified to the surface of g-C_3N_4. In Fig. 3(b), the high-resolution C1s spectra of Ag@g-C_3N_4 can be fitted into three peak components by Gaussian curve at binding energy about 284.4, 287.5 and 288.1 eV. Among them, the peak at 284.4 eV is ascribed to the surface adventitious carbon or typically attributed to the C bond (C–C and C=C), that at 287.5 eV corresponds to the C–O environment, and the sp^2-bond C in tri-s-triazine structure rings (N–C=N) is responsible for the peak at 288.1 eV[19]. In Fig. 3c, two peaks of N 1s were centered at 398.3 and 400.0 eV, which were attributed to sp^2 C=N–C bond in the tri-s-triazine ring and tertiary N bonded to C atoms (N–$(C)_3$), respectively[20]. The Ag 3d XPS spectra in Fig. 3(d) show the two major peaks at 367.6 and 373.8 eV, which can be attributed to the binding energies of Ag3$d_{5/2}$ and Ag3$d_{3/2}$, respectively. The Ag 3d can be fitted into four peaks, in which the two peaks at 367.4 and 374.0 eV with splitting distance of 6 eV were caused by Ag(0), indicating the formation of metallic Ag on the surface of g-C_3N_4[21]. The XPS results further confirmed the successful deposition of Ag nanoparticles on the surface of g-C_3N_4.

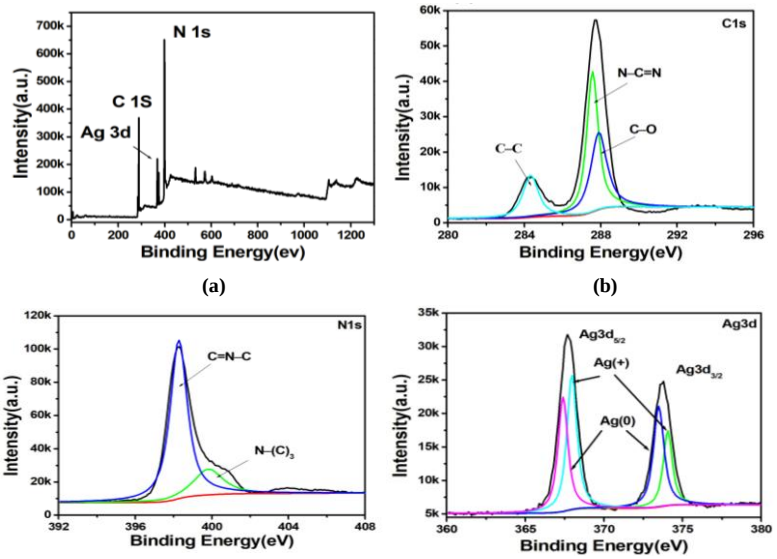

Fig. 3. (a) XPS survey of pristine Ag@g-C_3N_4, XPS spectra for (b) C1s, (c) N1s, (d) Ag3d

The specific surface area of Ag@g-C_3N_4 sample is larger than that before modification. The adsorption types of the two materials before and after Ag modification can be classified as V type, the pore volume is basically unchanged, and the pore size distribution is in the range of 2∼50 nm with mesopore structure. It is worth mentioning that the pore size distribution of the modified materials is more diversified. Large specific surface area and diversified pore size distribution are helpful to increase the catalytic active sites, and then improve their catalytic reduction activity.

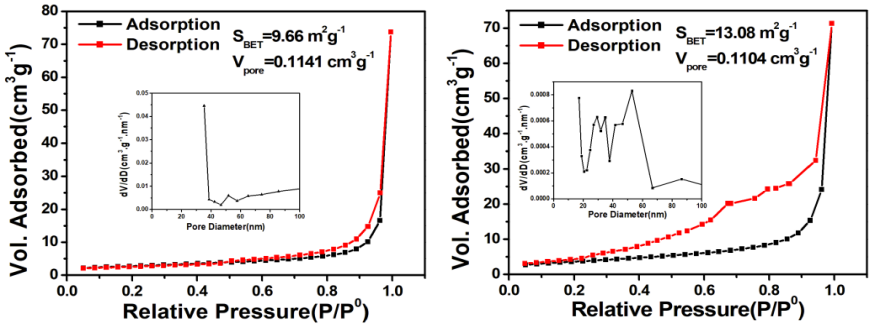

Fig. 4. N_2 adsorption-desorption curves and pore size distribution of (a) g-C_3N_4, (b) Ag@g-C_3N_4

In this work, the conversion of 4-NP to 4-AP catalyzed by Ag@*g*-C_3N_4 in the presence of $NaBH_4$ served as a model reaction to assess the catalytic reduction performance. As shown in Fig. 5a, the maximum absorption wavelength of the initial 4-NP aqueous solution is 317 nm, whereas it shifts to 400 nm when the $NaBH_4$ aqueous solution is added to the 4-NP aqueous solution due to the formation of 4-NP anions; on the other hand, the maximum absorption wavelength of 4-NP's reductive product 4-AP is around at 300 nm. Therefore, the extent of 4-NP reduction reaction can be traced by a decrease of absorbance at 400 nm and an increase of absorbance at 300 nm.

From Fig. 5b, with the help of *g*-C_3N_4 catalyst, the absorption intensity of 4-NP at 400 nm decreases with reaction time, but nearly no new peak is formed simultaneously, which indicated that only the adsorption process occurs, and almost no catalytic reduction effect to the 4-NP is found. However, with the aid of catalyst Ag@*g*-C_3N_4, the absorption intensity of 4-NP at 400 nm decreases quickly with time, accompanied by the appearance of the new peaks of 4-AP at around 300 nm (Fig. 5c), indicating that there is a conversion of 4-NP to 4-AP, and the catalytic efficiency of 92.2% within 10 min was obtained. The reduction reaction at given reaction follows pseudo first-order kinetics equation over the as-prepared Ag@*g*-C_3N_4 catalyst. As shown in Fig. 5d, the equation is $\ln(A_t/A_0) = 0.03045 - 0.26427t$, $R^2 = 0.9977$. The comparative experimental results show Ag nano-particles loaded on the surface of *g*-C_3N_4 can effectively improve its catalytic reduction activity. This study is of great significance for the effective reduction of 4-NP through the catalyst prepared by simple green process.

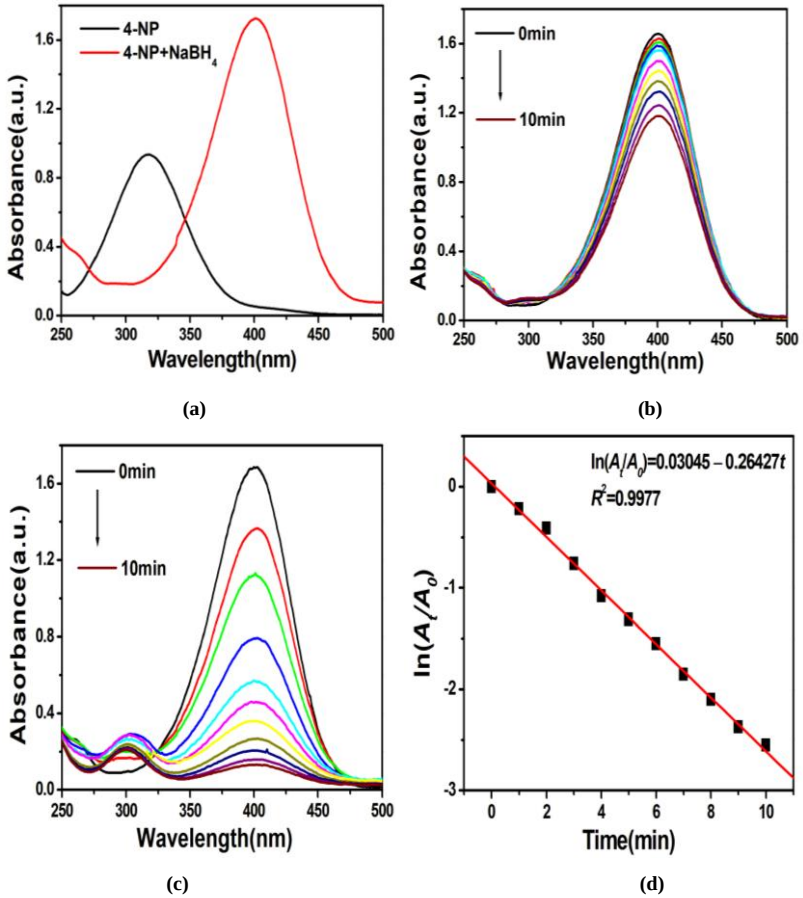

Fig. 5. UV-vis spectra of (a) 4-NP and 4-NP + $NaBH_4$; 4-NP reduction with (b) *g*-C_3N_4, (c) Ag@*g*-C_3N_4; (d) pseudo first order reaction kinetics of Ag@*g*-C_3N_4

In addition to excellent catalytic properties, good stability and repeatability were also required for the catalyst. Fig. 6 shows the result of the cyclic performance of the Ag@*g*-C_3N_4 catalyst. The catalyst is recycled for 3 times and its catalytic efficiency is kept at 95%. Thus result indicated that the catalyst has good cycle stability and is expected to be used in the actual catalytic process.

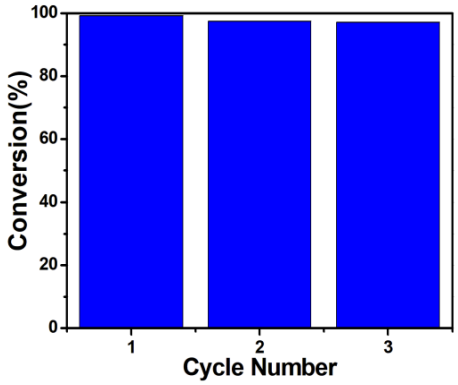

Fig. 6. Reusability of Ag@*g*-C_3N_4 in successive cycles

4 CONCLUSION

In this study, Ag@*g*-C_3N_4 composite has been successfully prepared by a simple liquid-phase deposition method and those characterizations through XRD, FT-IR, SEM, EDX elemental mapping, BET and XPS were also studied in detail. As a heterogeneous catalyst, the Ag@*g*-C_3N_4 composite has significant catalytic activity for the reduction of 4NP to 4-AP, and it can be reduced completely within 10 min. The reduction reaction at given reaction follows pseudo first-order kinetics equation using the as-prepared catalyst, in which the equation is $\ln(A_t/A_0) = 0.03045 - 0.26427t$, $R^2 = 0.9977$ and the apparent rate constant $K_{app} = 264.27 \times 10^{-3}$ min^{-1}. The Ag@*g*-C_3N_4 catalyst also has excellent cyclic catalytic stability. This study has important scientific research value and practical significance for the preparation of novel catalysts and effective catalytic reduction of organic pollutants.

REFERENCES

(1) Harika, V. K.; Sadhanala, V. K.; Perelshtein, I.; Gedanken, A. Sonication-assisted synthesis of bimetallic Hg/Pd alloy nanoparticles for catalytic reduction of nitrophenol and its derivatives. *Ultrason. Sonochem*. **2020**, 60, 1–9.

(2) Zhao, Y.; Wu, Z.; Wang, Y.; Yang, C.; Li, Y. Facile fabrication of polystyrene microsphere supported gold-palladium alloy nanoparticles with superior catalytic performance for the reduction of 4-nitrophenol in water. *Eng. Asp*. **2017**, 529, 417–424.

(3) Song, L.; Shu, L.; Wang, Y.; Zhang, X. F.; Wang, Z.; Feng, Y.; Yao, J. Metal nanoparticle-embedded bacterial cellulose aerogels *via* swelling-induced adsorption for nitrophenol reduction. *Int. J. Biol. Macromol*. **2020**, 143, 922–927.

(4) Afzal, S.; Julkapli, N, M.; Mun, L. K. Response surface approach for visible light assisted photocatalytic degradation of ortho nitrophenol by magnetically separable TiO_2/CS nanocomposite. *Mat. Sci. in Semicon. Proc.* **2019**, 99, 34–43.

(5) Wang, Z. M.; Zheng, M.; Xie, Y. B.; Li, M. M.; Zeng, M.; Cao, H. B.; Guo, L. Molecular dynamics simulation of ozonation of *p*-nitrophenol at room temperature with ReaxFF force field. *Acta Phys.-Chim. Sin*. **2017**, 33, 1399–1410.

(6) Alula, M. T.; Lemmens, P.; Madiba, M.; Present, B. Synthesis of free-standing silver nanoparticles coated filter paper for recyclable catalytic reduction of 4-nitrophenol and organic dyes. *Cellulose* **2020**, 27, 2279–2292.

(7) Liu, J.; Yan, X.; Wang, L.; Kong, L.; Jian, P. Three-dimensional nitrogen-doped graphene foam as metal-free catalyst for the hydrogenation reduction of *p*-nitrophenol. *Colloid Interface Sci*. **2017**, 497, 102–107.

(8) Wang, X.; Song, J.; Lu, J.; Zhu, W.; Hu, G. Development of a Z-scheme Ag/Ag_2WO_4/*g*-C_3N_4 photocatalyst for RhB fast degradation assisted with H_2O_2. *J. Mater. Sci-Mater. El.* **2021**, 8, 1–14.

(9) Roselin, L. S.; Patel, N.; Khayyat, S. A. Codoped *g*-C_3N_4 nanosheet for degradation of organic pollutants from oily wastewater. *Appl. Surf. Sci*. **2019**, 494, 952–958.

(10) Yu, C.; Wang, P.; Wang, X.; Chen, F.; Yu, H. Silver-melamine nanowire-assisted synthesis of net-like AgCl-Ag/*g*-C_3N_4 for highly efficient photocatalytic degradation ability. *J. Alloy. Compd*. **2019**, 806, 263–271.

(11) Zhao, X.; Zhang, X.; Han, D.; Liu, L. Ag supported Z-scheme $WO_{2.9}$/*g*-C_3N_4 composite photocatalyst for photocatalytic degradation under visible light. *Appl. Surf. Sci*. **2020**, 501, 144258.1–144258.9.

(12) Wang, X.; Tan, F.; Wang, W.; Qiao, X.; Qiu, X.; Chen, J. Anchoring of silver nanoparticles on graphitic carbon nitride sheets for the synergistic

catalytic reduction of 4-nitrophenol. *Chemosphere* **2017**, 172, 147–154.

(13) Liu, X.; Tang, R. Y.; Xia, X. M.; Qin, Y. Y. The study of visible-light photocatalytic degradation activity of Ag doped *g*-C_3N_4 obtained by heating process. *Mater. Res. Express* **2020**, 7, 1–11.

(14) Xue, J.; Ma, T.; Shen, Q.; Guan, R.; Jia, H.; Liu, X.; Xu, B. A novel synthesis method for Ag/*g*-C_3N_4 nanocomposite and mechanism of enhanced visible-light photocatalytic activity. *J. Mater. Sci-Mater. El.* **2019**, 30, 15636–15645.

(15) She, P.; Li, J.; Bao, H.; Xu, X.; Hong, Z. Green synthesis of Ag nanoparticles decorated phosphorus doped *g*-C_3N_4 with enhanced visible-light-driven bactericidal activity. *J. Photochem. Photobiol. A Chem.* **2019**, 384, 11028–11028.

(16) Yang, Z.; Xu, X.; Liang, X.; Lei, C.; Cui, Y.; Wu, W.; Yang, Y.; Zhang, Z.; Lei, Z. Construction of heterostructured MIL-125/Ag/*g*-C_3N_4 nanocomposite as an efficient bifunctional visible light photocatalyst for the organic oxidation and reduction reactions. *Appl. Catal. B: Environ.* **2017**, 205, 42–54.

(17) Min, C.; Shen, C.; Li, R.; Li, Y.; Qin, J.; Yang, X. In-situ fabrication of Ag/*g*-C_3N_4 composite materials with improved photocatalytic activity by coordination-driven assembly of precursors. *Ceram. Int*. **2016**, 42, 5575–5581.

(18) Jin, J.; Liang, Q.; Ding, C. Y.; Li, Z. Y.; Xu, S. Simultaneous synthesis-immobilization of Ag nanoparticles functionalized 2*D* *g*-C_3N_4 nanosheets with improved photocatalytic activity. *J. Alloys. Compd.* **2017**, 691, 763–771.

(19) Chen, M.; Guo, C.; Hou, S.; Wu, L.; Lv, J.; Hu, C.; Zhang, Y.; Xu, J. In-situ fabrication of Ag/Pg-C_3N_4 composites with enhanced photocatalytic activity for sulfamethoxazole degradation. *J. Hazard. Mater*. **2019**, 366, 219–228.

(20) Wei, F.; Li, J.; Dong, C.; Bi, Y.; Han, X. Plasmonic Ag decorated graphitic carbon nitride sheets with enhanced visible-light response for photocatalytic water disinfection and organic pollutant removal. *Chemosphere* **2020**, 242, 1–11.

(21) Liang, C.; Guo, H.; Zhang, L.; Ruan, M.; Niu, C. G.; Feng, H. P.; Wen, X. J.; Tang, N.; Liu, H. Y.; Zeng, G. M. Boosting molecular oxygen activation ability in self-assembled plasmonic p-n semiconductor photocatalytic heterojunction of WO_3/Ag@Ag_2O. *Chem. Eng. J*. **2019**, 372, 12–25.